



OPEN Dioscin from smilax china rhizomes inhibits platelet activation and thrombus formation via up-regulating cyclic nucleotides

Ga Hee Lee¹, Jin Pyo Lee¹, Na Yoon Heo¹, Chang-Dae Lee², Gyeongchan Kim³, Akram Abdul Wahab⁴, Man Hee Rhee^{4,5}, Sanghyun Lee^{2,6}✉ & Dong-Ha Lee^{1,7}✉

Cardiovascular disease, the leading cause of mortality in the United States, is caused by abnormal platelet accumulation and coagulation. Dioscin has been reported to suppress the growth of tumor-associated cells and trigger apoptosis. However, its mechanism in inhibiting platelet activation has not been confirmed. This study investigates whether dioscin from *Smilax china* rhizomes exerts antithrombotic effects by regulating the activation of human platelets and explains its mechanism of action. Dioscin increased the production of cyclic adenosine monophosphate (cAMP) and cyclic guanosine monophosphate (cGMP). This increase induced the phosphorylation of inositol 1,4,5-triphosphate receptor (IP₃R), which inhibited the dense Ca²⁺ release channels, thereby reducing Ca²⁺ mobilization. Furthermore, it promoted the phosphorylation of vasodilator-stimulated phosphoprotein (VASP), which suppressed integrin α IIb β ₃ and fibrinogen binding, thus inhibiting platelet activation. Dioscin regulated phosphorylation of phosphatidylinositol 3-kinase (PI3K)/protein kinase B (Akt), mitogen-activated protein kinase (MAPK) and cytosolic phospholipase A₂ (cPLA₂), which are proteins associated with platelet granule release. Finally, ingestion of *S. china* rhizomes containing dioscin significantly inhibited thrombus formation in the FeCl₃-induced thrombosis model. Therefore, dioscin from *S. china* rhizomes exhibited antiplatelet effects that could delay or halt thrombus formation by regulating the phosphorylation of various signaling molecules and related proteins, thus suggesting dioscin's potential value for development as an antithrombotic agent.

The World Health Organization (WHO) reported that in 2019, cardiovascular disease (CVD) accounted for the highest number of deaths worldwide, with 8.9 million people losing their lives. The American Heart Association estimated that there will be 19.05 million deaths from CVD by 2023, representing a staggering 19.8% increase from 2010¹. When blood vessels are damaged, platelets act hemostatically to prevent bleeding. However, when platelets are produced in excess and clump together, they can lead to blood clot formation, which contributes to the onset of cardiovascular complications, including conditions where arteries harden, blood flow to the heart is blocked, or the brain is deprived of oxygen, potentially resulting in heart failure or stroke. Therefore, regulating platelet activity is crucial to prevent and treat platelet aggregation.

Endothelial cells in vascular tissues release prostaglandin I₂ and nitric oxide, triggering the production of cAMP and cGMP in platelets under normal blood flow conditions. The rise in cAMP activates protein kinase A (PKA), while protein kinase G (PKG) is activated by cGMP. Phosphorylated vasodilator-stimulated phosphoprotein (VASP) and inositol 1,4,5-triphosphate receptor (IP₃R) are involved in promoting antiplatelet responses². The phosphorylation of IP₃R decreases Ca²⁺ influx into the cytoplasm through the dense tubular system³. VASP, a key substrate for both PKG and PKA, plays a critical role in regulating α IIb β ₃ integrin function and actin cytoskeleton reorganization^{4,5}.

¹Department of Biomedical Laboratory Science, Namseoul University, Cheonan 31020, Republic of Korea.

²Department of Plant Science and Technology, Chung-Ang University, Anseong 17546, Republic of Korea.

³Department of Health Administration and Management, Soonchunhyang University Graduate School, Asan 31538, Republic of Korea. ⁴Department of Veterinary Medicine, College of Veterinary Medicine, Kyungpook National University, Daegu 41566, Republic of Korea. ⁵Institute for Veterinary Biomedical Science, College of Veterinary Medicine, Kyungpook National University, Daegu 41566, Republic of Korea. ⁶Natural Product Institute of Science and Technology, Anseong 17546, Republic of Korea. ⁷Molecular Diagnostics Research Institute, Namseoul University, Cheonan 31020, Republic of Korea. ✉email: slee@cau.ac.kr; dhlee@nsu.ac.kr

The release of serotonin and adenosine triphosphate (ATP) from granules within platelets is an essential step that promotes aggregation. This process is driven by the phosphorylation of both mitogen-activated protein kinases (MAPKs) and PI3K/Akt pathways, which play vital roles⁶. MAPKs, including subtypes such as p38, JNK, and ERK, are involved in intracellular signaling that regulates clot formation and thrombus growth⁷. Present in human platelets, the MAPK pathway facilitates the secretion of granules by acting as a crucial intermediary for signaling^{8–13}. Activation of MAPK leads to phosphorylation of cytosolic phospholipase A₂ (cPLA₂), which is a membrane-associated enzyme responsible for increasing the production of thromboxane A₂ (TXA₂), further driving aggregation and platelet activation^{13,14}. Simultaneously, the PI3K/Akt pathway enhances aggregation by boosting the secretion of dense granules¹⁵.

Dioscin is a steroidal saponin derived from *Smilax china* rhizomes, known for its ability to inhibit tumor growth and induce cell death (apoptosis) in cancer cells of the prostate, as well as in tumor-associated macrophages found in lung cancer and osteosarcoma stem cells, primarily through the MAPK pathway^{16–18}. It has also been suggested that dioscin exhibits lipid-lowering, anticancer, anti-inflammatory, and hepatoprotective properties, and it induces cancer cell autophagy¹⁹. However, most studies have focused on cancer cells or immune system cells, and little research has been done on the antiplatelet mechanisms of dioscin in human platelet cells. Thus, this study sought to explore how dioscin from *S. china* rhizomes inhibits human platelet aggregation and contributes to the creation of antithrombotic agents.

Material and methods

Plant materials and sample preparation

S. china rhizomes were collected from Chungju, Chungbuk Province, Korea, and authenticated by Prof. J. H. Kwak, Sungkyunkwan University, Suwon, Korea. A voucher specimen of rhizomes (No. LEE2023-1001) has been deposited in the herbarium of the Department of Plant Science and Technology, Chung-Ang University, Anseong, Korea. After air-drying in the shade for 15 days, the rhizomes were then subjected to ethanol extraction using a reflux extractor for 5 h. The resulting extracts were filtered and then concentrated using a rotary evaporator to obtain concentrated ethanol extracts.

High-performance liquid chromatography (HPLC)/evaporative light scattering detector (ELSD) analysis

The HPLC/ELSD analysis was carried out with a Waters Alliance e2695 separations module (Waters Co., Milford, MA, USA) as the HPLC system. A YMC Pack-Pro C18 column (dimensions: 4.6 × 250 mm, 5 μm) from YMC Co. (Kyoto, Japan) was employed, following the method outlined in a previous study²⁰. Dioscin was sourced from the Natural Product Institute of Science and Technology (www.nist.re.kr), Anseong, Korea.

Preparation of human platelet suspension

Human platelet-rich plasma (PRP) collected from healthy volunteers who gave informed consent was obtained from the Korean Red Cross Blood Center (KRBC, Suwon, Korea). They are an authorized institution responsible for the separation and preparation of blood donors in Korea and provide stable blood samples in accordance with the Blood Management Act. The study protocol received clearance from the Institutional Review Board (IRB) under the Bioethics Review Committee of Namseoul University (1,041,479-BR-202208–005). The human platelet suspensions were prepared according to the method performed previously²¹. The PRP was spun in a centrifuge at a force of 1,610 × g for 8 min, followed by two washes with a buffer at pH 6.9, and the resuspended pellets were prepared using a suspension buffer at pH 7.4. All processes were carried out at ambient temperature, and platelet suspensions were adjusted to reach a cell concentration of 10⁸ cells per milliliter.

Platelet aggregation assay

To evaluate platelet aggregation, dioscin was prepared at various concentrations and mixed with human platelet suspension (10⁸ cells/mL). CaCl₂ was added to reach 2 mM CaCl₂, and the mixture was incubated at 37 °C for 3 min with a stirrer bar rotating at 1000 rpm. After that, platelet agonists were added individually to stimulate platelet aggregation, and the aggregation formation process was monitored with continuous stirring for 5 min, and the aggregation rate was determined by the change in light transmittance using an aggregometer (Chrono-Log Co., Havertown, PA, USA). Dioscin was dissolved in dimethyl sulfoxide to a final concentration of 0.1%, and the control group was tested by containing the same concentration of dimethyl sulfoxide.

Cytotoxicity assay

To assess the cytotoxicity of dioscin, lactate dehydrogenase release from the cytoplasm of platelets was measured. Human platelet suspensions (10⁸ cells/mL) were exposed to varying concentrations of dioscin for 1 h, followed by centrifugation at 10,000 × g for 2 min. The supernatant was analyzed to evaluate cytotoxicity with an ELISA instrument (TECAN, Salzburg, Austria).

Experiment to measure intracellular calcium concentration

A mixture of fura 2-AM (5 μM) and PRP was subjected to incubation at 37 °C for a period of 60 min. Afterward, human platelet suspensions (10⁸ cells/mL) were rinsed with a wash buffer. Following the wash, the platelets were resuspended in suspension buffer and incubated again for 3 min at 37 °C, either in the presence or absence of the test substance. Platelet activation was triggered by U46619 (0.5 μM) combined with 2 mM CaCl₂, and the platelets were incubated with U46619 for 5 min. To quantify [Ca²⁺]_i, fluorescence measurements of fura 2-AM were taken using a spectrofluorometer (Hitachi F-7000, Tokyo, Japan) following the method outlined by Grynkiewicz²².

Experiments to measure ATP, serotonin and TXA₂

Platelet suspensions (10^8 cells/mL) were treated with dioscin and incubated at 37 °C for 3 min. Then, 2 mM CaCl₂ was added and stimulated with U46619 for 5 min. The ATP and serotonin release reactions were stopped by adding ice-cold 2 mM EDTA. After centrifugation, the supernatant was collected for further analysis. ATP levels were quantified using Cayman ATP Detection Assay Kit (Cayman Chemical, Ann Arbor, MI, USA) with measurements taken using a chemiluminescence reader. Serotonin levels were quantified using Serotonin ELISA Kit (Abcam, Cambridge, UK), with detection at a wavelength of 410 nm using the ELISA reader (TECAN, Salzburg, Austria). TXA₂ levels were quantified using TXB₂ ELISA Kit (Cayman Chemical, Ann Arbor, MI, USA), with detection at a wavelength of 410 nm using the ELISA reader (TECAN, Salzburg, Austria).

P-selectin expression analysis

Platelet suspensions (10^8 cells/mL) were treated with dioscin and incubated at 37 °C for 3 min. Subsequently, CaCl₂ was added to achieve a final concentration of 2 mM, followed by stimulation with U46619 for 5 min. After stimulation, all reagents and samples were transferred to light-protected tubes. For fluorescent antibody staining, Anti-P-Selectin (CD62P), Alexa Fluor 488 (5 µL) was added, and the samples were incubated at room temperature for 1 h in the dark²³. The stained samples were then transferred to tubes equipped with a cell strainer to remove debris. Subsequently, 0.5% paraformaldehyde was added at a 1:1 ratio to fix the cells. The level of P-Selectin expression was assessed by measuring fluorescence intensity using a flow cytometer (BD Biosciences, San Jose, CA, USA), and data analysis was performed with CellQuest software (BD Biosciences).

Western immunoblotting measurement

The aggregate formation of platelets was carried out for 5 min, after which it was halted through the introduction of a lysis buffer. The resulting lysates from the platelets were measured using a BCA protein assay kit (Pierce Biotechnology, IL, USA). In preparation for western blot analysis, 15 µg of protein from the lysates underwent separation through an 8% SDS-PAGE gel and was then transferred onto a PVDF membrane. The membrane was incubated with a primary antibody at a 1:1,000 dilution, followed by a secondary antibody at a 1:10,000 dilution. Protein bands were visualized and analyzed using Quantity One Version 4.5 software (BioRad, Hercules, CA, USA).

Fibrinogen binding measurement experiments for αIIbβ₃

Platelet suspensions (10^8 cells/mL) were incubated with the appropriate reagents and exposed to 30 µg/mL fibrinogen labeled with Alexa Fluor 488 at a temperature of 37 °C for a duration of 5 min. To stabilize the interaction between the platelets and the Alexa Fluor-conjugated fibrinogen, 0.5% paraformaldehyde was introduced to pre-chilled PBS. All steps were carried out in darkness to prevent light interference. The binding of fibrinogen to integrin αIIbβ₃ was assessed through fluorescence using a flow cytometer (BD Biosciences, San Jose, CA, USA), and data analysis was completed using CellQuest software (BD Biosciences).

cAMP and cGMP measurement

Human platelets (10^8 cells/mL) were washed and incubated for 3 min at 37 °C, in the presence or absence of 2 mM CaCl₂. Afterward, U46619 (0.5 µM) was used to trigger platelet aggregation over a 5-min period. To stop the aggregation and stabilize the samples, 80% cold ethanol was added to the reaction mixture. The supernatants were then collected by centrifugation, and the cAMP and cGMP concentrations in the samples were measured using the cAMP and cGMP ELISA Kits from TECAN (Salzburg, Austria), with absorbance measured at 410 nm using the ELISA reader (TECAN, Salzburg, Austria).

Platelet-mediated clot retraction assay

A volume of 300 µL of human PRP was transferred into polyethylene tubes and incubated at 37 °C for 15 min, either in the presence or absence of dioscin. To initiate thrombus contraction, thrombin (0.05 Unit/mL) was introduced. Photographs of the fibrin clot formation were captured every 15 min using a digital camera. The clotting area was then quantified with ImageJ software (v1.46, U.S. National Institutes of Health).

Ethical statement

The Animal Experimental Ethics Committee approved the study involving Sprague–Dawley (SD) rats. All animal experiments were conducted in accordance with established guidelines and were approved by the Animal Care Committee of Namseoul University, South Korea (Permit no. NSU-2024–02). The animals were placed in a CO₂ chamber, and euthanasia was induced by injecting 20% CO₂. Death was confirmed by respiratory arrest, no heartbeat, and unresponsiveness. The study was reported following the ARRIVE guidelines, and all methods complied with relevant guidelines and regulations.

In vivo FeCl₃-induced thrombosis model

Seven-week-old male SD rats weighing 240–260 g were provided by Koatech (Pyeongtaek, Korea) and used the in vivo FeCl₃-induced thrombosis model. The rats were randomly divided into five groups (n = 5/group): the control group (saline), three experimental groups (50 mg/kg, 100 mg/kg, and 200 mg/kg of *Smilax china* rhizomes extract), and the positive control group (30 mg/kg of aspirin). Each group was housed in a single cage. The animals were acclimated under environmentally controlled conditions of 23 ± 2 °C, 50% ± 10% relative humidity, and a 12-h light–dark cycle.

In vivo FeCl₃-induced blood flow measurement

SD rats were orally administered saline, aspirin (ASA), or *Smilax china* rhizomes extract containing dioscin (SR) for seven days to evaluate the development of FeCl₃-induced thrombosis. One hour after the final treatment, the SD rats were anesthetized with an intraperitoneal injection of Avertin and maintained at 37 °C on a heating pad. After separating the fat, fascia, and surrounding tissue, the left carotid artery was identified, and a flow probe was placed over the artery in each experimental group to measure blood flow. After a 5-min baseline measurement, a piece of FeCl₃ (35%)-soaked filter paper (10 mm × 3 mm) was wrapped around the area beneath the laser probe to induce thrombosis. Occlusion time was recorded while monitoring blood flow for a total of 30 min.

Statistical analysis

The experimental results were reported as the mean along with the standard deviation (SD) based on the number of observations. To determine significant differences between the groups, we conducted an analysis of variance (ANOVA) and applied the Tukey–Kramer method for post-hoc comparisons. Statistical assessments were performed using SPSS 21.0.0.0 software (SPSS, Chicago, IL, USA), with statistical significance established at $p < 0.05$.

Results

Content of dioscin in *Smilax china* rhizomes by HPLC/ELSD analysis

The purity of dioscin was 99% (Fig. 1A). The retention time of dioscin in the HPLC/ELSD chromatogram was 40.3 min, and its concentration was determined to be 1.67 mg/g of extract (Fig. 1B).

Effects of dioscin on platelet aggregation and cytotoxicity

The evaluation of aggregation reactions in human platelets activated by U46619 (0.5 μM), thrombin (0.04 Unit/mL) and collagen (2.5 μg/mL) revealed that platelet aggregation reached 85.8% with U46619, 81.3% with thrombin and 80.3% with collagen, both showing a substantial aggregation response (Fig. 2). Dioscin demonstrated inhibition of platelet aggregation caused by U46619 in a manner proportional to the dose, with inhibition rates of 16.7% at 8 μM, 50.5% at 16 μM, 70.6% at 24 μM, and 95.0% at 32 μM (Fig. 2A). The half-maximal inhibitory concentration (IC₅₀) of dioscin was determined to be 13.82 μM (Fig. 2D), showing a potent inhibitory effect. Additionally, dioscin showed no cytotoxicity toward human platelets (Fig. 2E). Therefore, it was confirmed that dioscin strongly inhibits platelet aggregation triggered by U46619 (0.5 μM), thrombin (0.04 Unit/mL) and collagen (2.5 μg/mL) without causing cytotoxic effects. When dioscin was co-treated with PKA inhibitor (H-89 dihydrochloride) or PKG inhibitor (trifluoroacetate salt), and aggregation was induced with U46619 (0.5 μM), the aggregation rate induced by dioscin (24 μM) was restored by the PKA inhibitor (1 μM) or PKG inhibitor (100 μM) from 35.3% to 60.8% or 55.3%, respectively. This suggests that dioscin inhibits platelet activation through the cAMP/PKA and cGMP/PKG pathways (Fig. 2F,G).

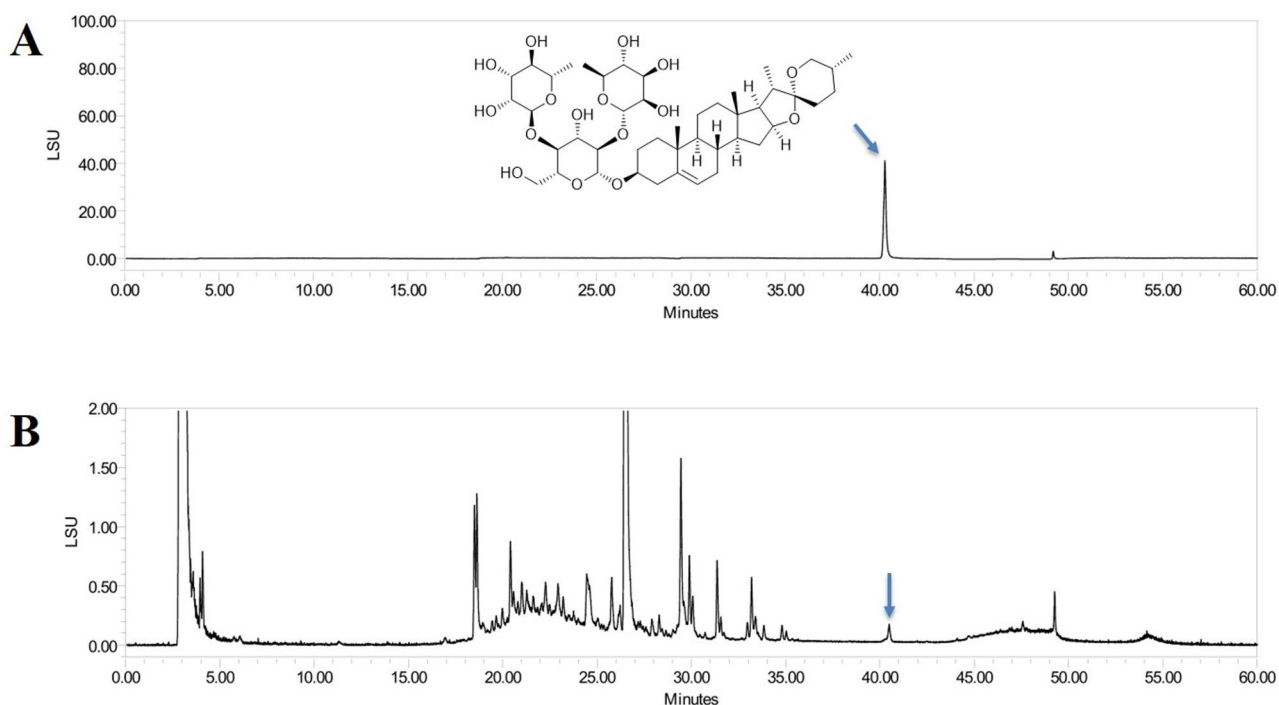


Fig. 1. HPLC/ELSD chromatograms. (A) Purity chromatogram of dioscin. (B) Extract chromatogram of *S. china* rhizomes.

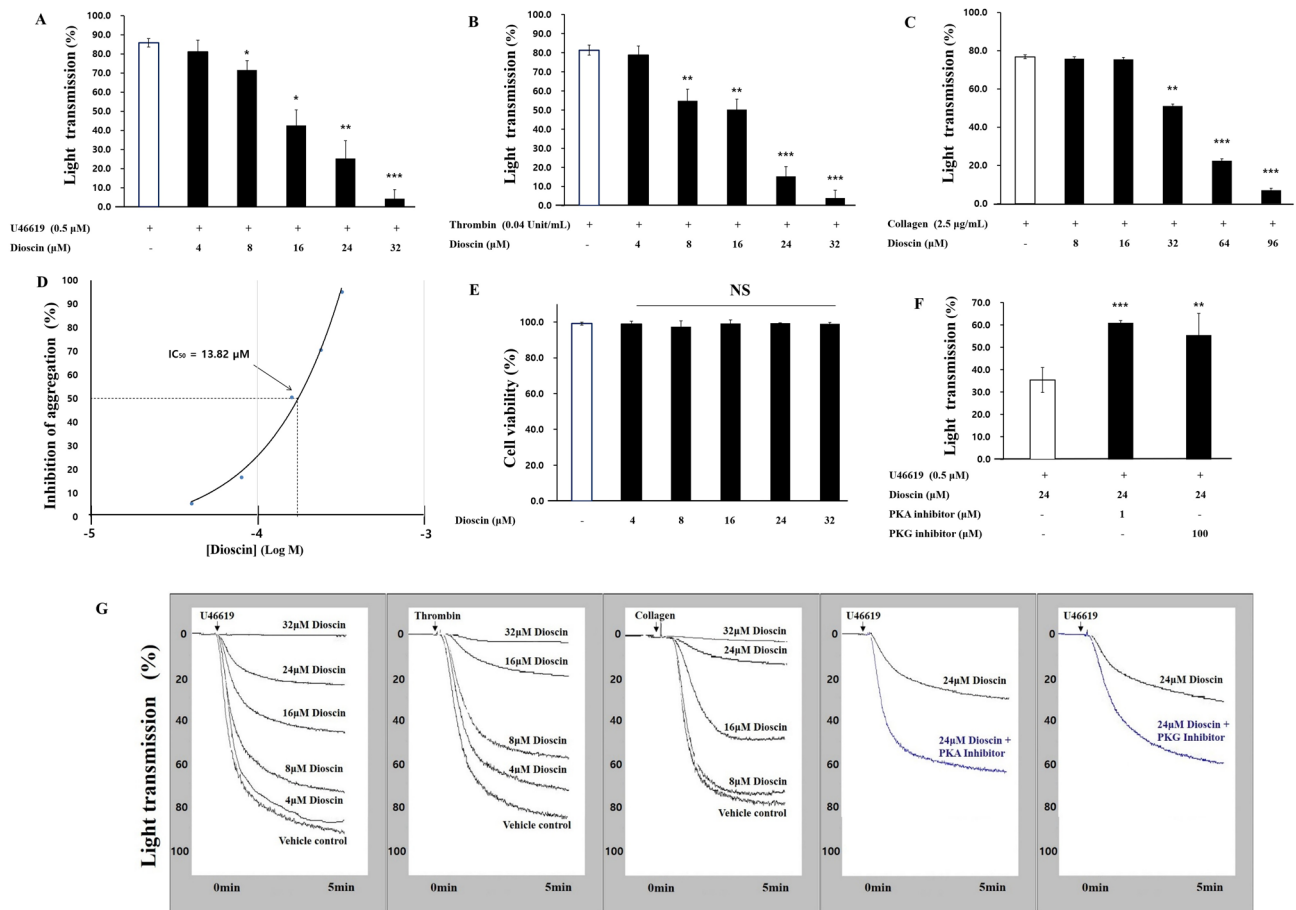


Fig. 2. The impact of dioscin on platelet aggregation induced by agonists. (A) The effect of dioscin on U46619-induced aggregation in human platelets. (B) The effect of dioscin on thrombin-induced aggregation in human platelets. (C) The effect of dioscin on collagen-induced aggregation in human platelets. (D) The IC_{50} value of dioscin on U46619-induced platelet aggregation. (E) Cytotoxicity of dioscin on suspended platelets. (F) The effect of dioscin on platelet aggregation after incubation with a PKA or PKG inhibitor for 3 min in human platelets. (G) The flow chart of dioscin on agonists-induced aggregation in human platelets. Data are presented as mean \pm SD ($n = 4$). Statistical significance is denoted by * $p < 0.05$, ** $p < 0.01$ and *** $p < 0.001$ when compared to agonist-stimulated platelets.

Effects of dioscin on cyclic nucleotide formation, intracellular Ca^{2+} migration, and IP_3R phosphorylation

The importance of cyclic nucleotides (cGMP and cAMP) in regulating platelet activation is well-known. In this study, dioscin's ability to boost cGMP and cAMP production was examined. Platelet activation induced by U46619 in the presence of dioscin showed a corresponding increase in cGMP and cAMP levels (Figs. 3A, B). These results indicate that dioscin disrupts platelet activation by elevating cGMP and cAMP concentrations in U46619-activated platelets. Additionally, pretreatment of platelets with dioscin led to significant phosphorylation of IP_3R (Fig. 3C), which aligned with a marked decrease in Ca^{2+} mobilization induced by U46619 when dioscin was present (Fig. 3D). These findings suggest that dioscin impedes Ca^{2+} mobilization by blocking Ca^{2+} channels through the phosphorylation of IP_3 receptors.

Investigation of dioscin's effect on VASP phosphorylation and fibrinogen binding

Building on the discovery that dioscin increases cAMP and cGMP levels in U46619-stimulated platelets, an assessment was conducted to determine whether it also impacts VASP, a key protein influenced by these cyclic nucleotides. As the concentration of dioscin increased, a corresponding concentration-dependent increase was observed in VASP phosphorylation at Ser¹⁵⁷, a site regulated by cAMP. Similarly, an increase was observed in Ser²³⁹ phosphorylation, a site affected by cGMP. This effect became especially prominent at dioscin concentrations exceeding 16 μ M. These findings suggest that dioscin-induced increases in cAMP and cGMP resulted in enhanced phosphorylation of Ser¹⁵⁷ (cAMP-dependent VASP) and Ser²³⁹ (cGMP-dependent VASP) (Fig. 4A). Given the role of dioscin in elevating cAMP/cGMP levels and stimulating phosphorylation at these key VASP sites, further analyses were conducted to explore its impact on the interaction between fibrinogen and $\alpha IIb\beta_3$. In the presence of U46619, fibrinogen binding to $\alpha IIb\beta_3$ increased to 92.1% (Fig. 4B, C). However, dioscin exhibited concentration-dependent inhibition of this binding, demonstrating its ability to elevate cAMP/

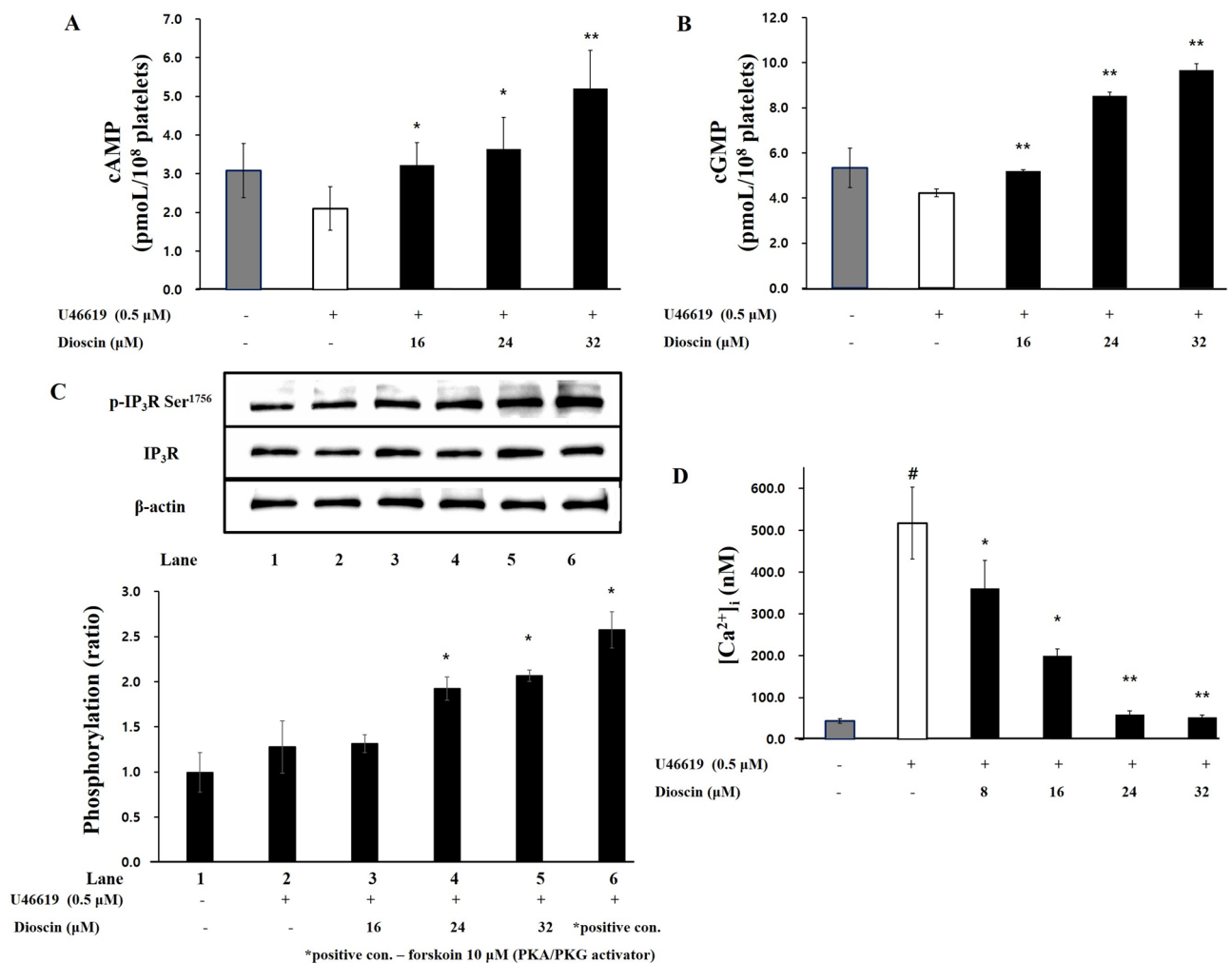


Fig. 3. Dioscin's impact on cAMP and cGMP production, intracellular calcium mobilization, and associated phosphoprotein levels. **(A)** Dioscin's influence on cAMP production. **(B)** Dioscin's influence on cGMP production. **(C)** Dioscin's influence in IP₃R phosphorylation. **(D)** Dioscin's influence on calcium mobilization inside platelets. Data are represented as mean ± SD (n = 4). Statistical significance is noted as #*p* < 0.05 for comparisons with unstimulated platelets, **p* < 0.05, ***p* < 0.01 and ****p* < 0.001 when compared to U46619-stimulated platelets.

cGMP levels and enhance VASP phosphorylation, which significantly reduced fibrinogen's binding affinity to αIIbβ₃.

Effects of dioscin on the phosphorylation of PI3K/Akt, MAPK, and cPLA₂

We also investigated how dioscin affects phosphorylation in the PI3K/Akt pathway, which is tied to the secretion of platelet granules. In platelets activated by U46619, both PI3K and Akt showed markedly increased phosphorylation levels. However, this effect was significantly diminished when treated with dioscin (Fig. 5A). Moreover, we examined dioscin's impact on mitogen-activated protein kinases (MAPKs), specifically p38 and JNK, which are crucial for platelet granule secretion and TXA₂ synthesis. Under U46619 stimulation, MAPK proteins exhibited heightened phosphorylation, but the presence of dioscin notably suppressed phosphorylation of p38 and JNK (Fig. 5B). In particular, in the case of ERK in MAPK, phosphorylation was not significantly caused by U46619, and the inhibitory effect by dioscin was not found. There is a result that the degree of inhibiting phosphorylation of ERK in substances inhibited platelet aggregation is weaker than that of JNK or p38²⁴. It has also been reported that the inhibition of ERK pathway has no effect on agonist-induced aggregation of human platelets²⁵. In this regard, it seems that further research is needed on how phosphorylation of ERK, JNK and p38 of MAPK is involved in the inhibition of aggregation of human platelets. Additionally, dioscin reduced cPLA₂ phosphorylation in a manner that correlated with dose (Fig. 5C). These results suggest that dioscin influences the phosphorylation of key proteins involved in U46619-stimulated platelet activation, including PI3K/Akt, MAPKs (p38 and JNK), and cPLA₂.

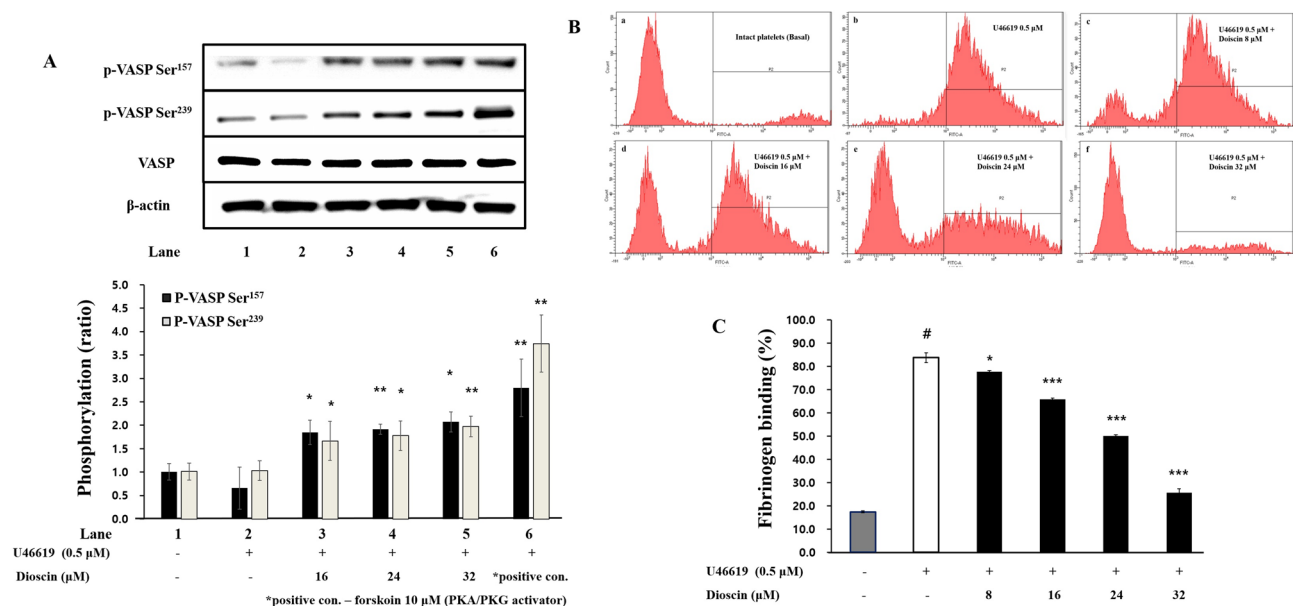


Fig. 4. The influence of dioscin on VASP phosphorylation and fibrinogen binding. **(A)** Dioscin's influence in regulating VASP phosphorylation. **(B)** The histogram from flow cytometry analysis of fibrinogen binding. a: Base (intact platelets), b: U46619, c: U46619 + dioscin (8 μM), d: U46619 + dioscin (16 μM), e: U46619 + dioscin (24 μM), f: U46619 + dioscin (32 μM). **(C)** The effect of dioscin on fibrinogen binding (%) induced by U46619. Data are presented as mean ± SD (n = 4). Statistical significance is indicated by #p < 0.05 compared to non-stimulated platelets, *p < 0.05, **p < 0.01 and ***p < 0.001 when compared to U46619-stimulated platelets.

Effects of dioscin on granule release

The discharge of ATP, serotonin and TXA₂ from granules inside platelets is a key factor in initiating platelet aggregation. This study investigated how dioscin affects this process. When platelets were activated with U46619 (0.5 μM), a significant increase in the release of ATP, serotonin and TXA₂ was observed. However, as dioscin concentrations increased, ATP, serotonin and TXA₂ levels decreased (Fig. 6). P-Selectin, which is released from alpha granules and induces platelet aggregation, was increased by U46619 stimulation but was found to be reduced upon dioscin treatment in dose-dependent. The findings suggest that dioscin's capacity to inhibit the release of granules is closely related to its effectiveness in limiting aggregate formation among platelets and the development of thrombosis.

Effect of dioscin on platelet-mediated fibrin coagulation

Platelets initiate fibrin clot formation through activation and aggregation, which is triggered by external signaling pathways. This study examined how dioscin influences fibrin clotting caused by thrombin-induced blood clot formation. The results demonstrated that thrombin-induced fibrin clotting led to thrombus development, and the introduction of varying doses of dioscin significantly decreased fibrin clot formation in a manner dependent on concentration (Fig. 7). These findings suggest that dioscin is a potent agent for inhibiting blood clot formation.

Smilax china rhizomes prevents thrombosis and regulates hemostasis

To assess the potential side effects of therapeutic agents on thrombosis and hemostasis, we established a FeCl₃-induced thrombus model, with aspirin serving as a positive control. Following thrombus induction using 35% FeCl₃, treatment with *Smilax china* rhizomes extract (SR) resulted in improved blood flow of rats in a dose-dependent manner (Fig. 8). In particular, significant results began to appear after 10 min, and results were steadily improved after 20 min, and the 100 mg/kg SR diet group showed effects similar to those observed in the 30 mg/kg aspirin diet group (Table 1).

Discussion

As far as we are aware, no prior studies have explored the mechanisms behind dioscin's antiplatelet activity in human platelet cells. Dioscin, a steroidal saponin derived from *S. china* rhizomes, has been reported to suppress tumor growth and trigger apoptosis in prostate cancer cells, lung cancer cells, and osteosarcoma stem cells, primarily through the MAPK (p38, ERK, and JNK) signaling pathway^{16–18}. In addition to its effects on cancer, dioscin has shown lipid-lowering, anti-inflammatory, anticancer, and hepatoprotective properties, as well as the ability to induce cancer cell autophagy¹⁹. These characteristics underscore the importance of further investigating its potential antiplatelet effects via the MAPK pathway.

When agonists activate platelets, phospholipase C₂ initiates the conversion of phosphatidylinositol 4,5-bisphosphate in the platelet membrane, resulting in diacylglycerol and inositol 1,4,5-trisphosphate (IP₃)

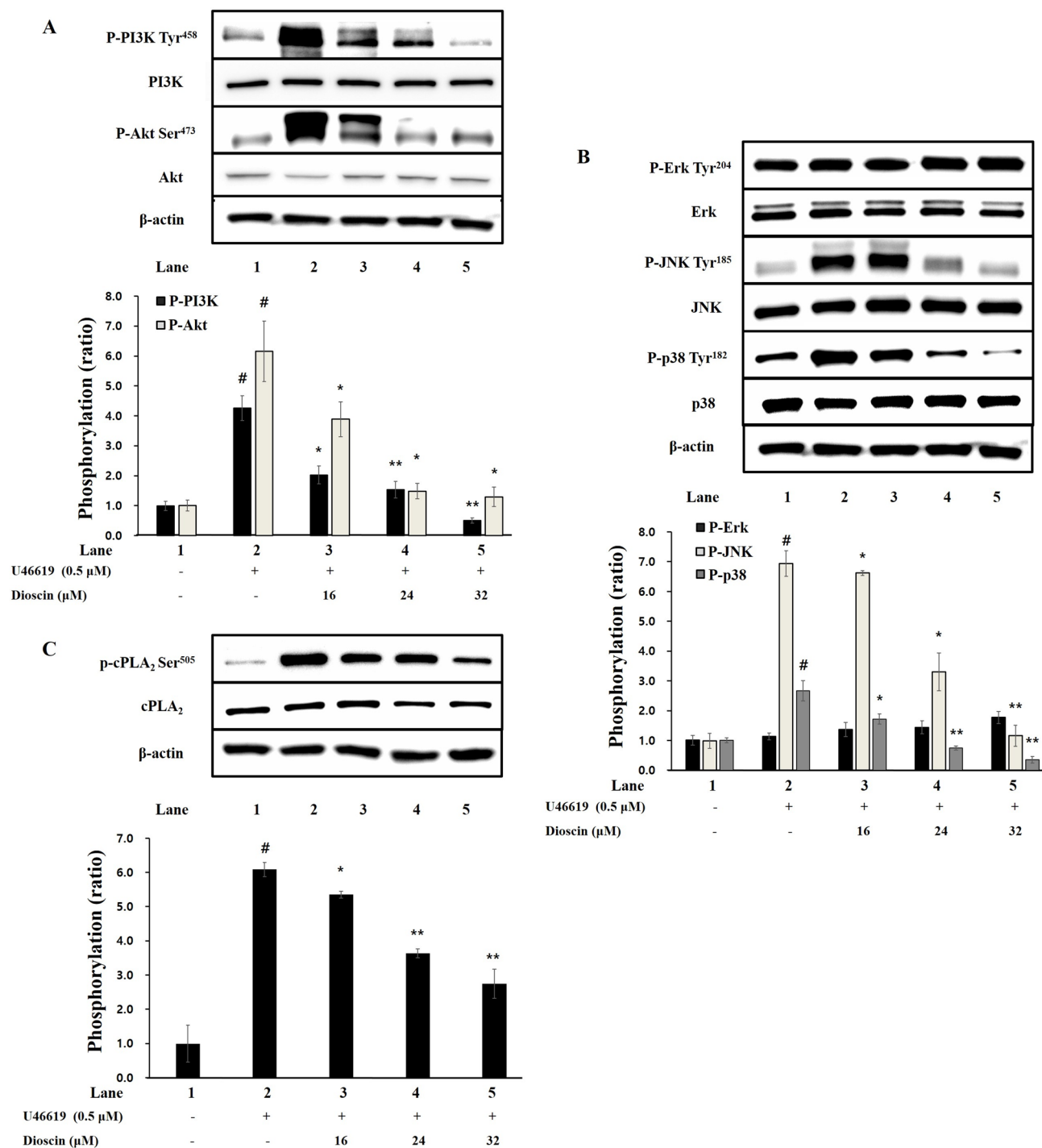


Fig. 5. Dioscin's influence on the phosphorylation of PI3K/Akt, MAPK, and cPLA₂. **(A)** Dioscin's effect on the phosphorylation of PI3K/Akt. **(B)** Dioscin's impact on MAPK phosphorylation. **(C)** Dioscin's role in the phosphorylation of cPLA₂. Data are presented as mean ± SD (n = 4). Statistical significance is indicated by #p < 0.05 when comparing with non-stimulated platelets, *p < 0.05, **p < 0.01 and ***p < 0.001 when compared to U46619-stimulated platelets.

creation²⁶. IP₃ then binds to its receptor (IP₃R), prompting calcium ions (Ca²⁺) to be released from the dense tubular system into the cytoplasm. This calcium influx drives the phosphorylation of key proteins like myosin light chain and pleckstrin, both of which are crucial for the aggregation of platelets²⁷.

Cyclic nucleotides, including cAMP and cGMP, act as inhibitors of calcium-induced platelet aggregation. This occurs by lowering intracellular calcium levels, primarily through the activation of protein kinases that are dependent on cyclic nucleotides, such as PKA and PKG²⁸. In this study, it was found that dioscin significantly increased cAMP and cGMP levels, which in turn reduced the release of intracellular calcium ([Ca²⁺]_i). Higher

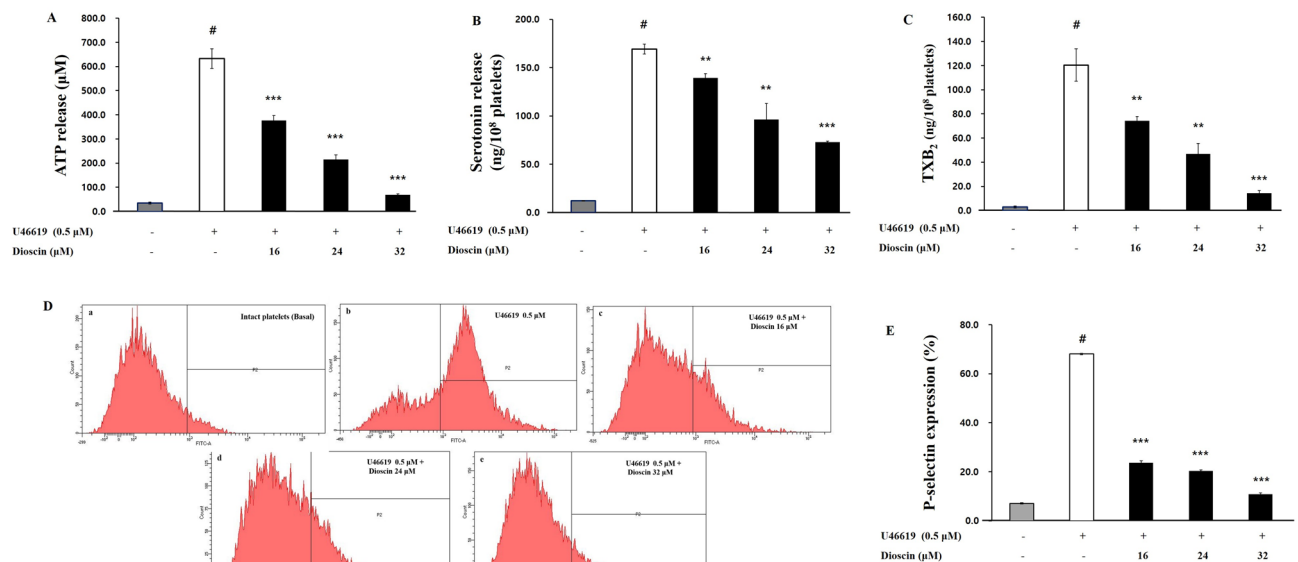


Fig. 6. Dioscin's influence on granule release. (A) Dioscin's effect on ATP secretion. (B) Dioscin's effect on serotonin secretion. (C) Dioscin's effect on TXA₂ production. (D) The histogram from flow cytometry analysis of P-selectin expression. a: Base (intact platelets), b: U46619, c: U46619 + dioscin (16 μM), d: U46619 + dioscin (24 μM), e: U46619 + dioscin (32 μM). (E) Dioscin's effect on p-selectin expression. Data are presented as mean ± SD (n = 4). Statistical significance is denoted by #p < 0.05 in comparison to non-stimulated platelets, *p < 0.05, **p < 0.01 and ***p < 0.001 when compared to U46619-stimulated platelets.

levels of cAMP and cGMP promote the activation of PKA, leading to the phosphorylation of multiple targets, including IP₃R²⁹. When PKA and PKG inhibitors were applied, the platelet aggregation that had been inhibited by dioscin was restored. This clearly demonstrates that dioscin exerts its inhibitory effect on platelet activation through the cAMP/PKA and cGMP/PKG pathways. Additionally, the results showed that dioscin enhances IP₃R phosphorylation in a dose-dependent fashion.

Dioscin activates the cAMP/PKA/IP₃R pathway, thereby reducing calcium levels within the cell. Additionally, the dioscin-induced increase in cAMP and cGMP production enhanced VASP phosphorylation through PKA and PKG activation. These VASP proteins, which bind to actin and profilin, play key roles in inhibiting platelet secretion and adhesion. VASP phosphorylation suppresses the activation of integrin αIIbβ₃, ultimately reducing platelet aggregation^{30,31}.

This study discovered that dioscin decreased fibrinogen binding to the αIIbβ₃ integrin, likely due to its ability to regulate fibrinogen attachment by activating the cAMP (or cGMP)/PKA (or PKG)/VASP pathway, which results in VASP phosphorylation at Ser¹⁵⁷ and Ser²³⁹. However, additional research is necessary to fully understand the precise mechanism by which dioscin elevates cAMP and cGMP levels. One possible explanation is that these cyclic nucleotides are dependent on the activation of cyclase (adenyl/guanyl) and phosphodiesterase (PDE)³². Inhibition of PDE during platelet aggregation markedly increases cyclic nucleotide levels, a significant observation, as PDE inhibitors have been shown to effectively treat thrombosis³³. Commonly used PDE inhibitors, such as dipyridamole and cilostazol, have demonstrated clinical efficacy by raising circulating nucleotide levels³⁴. Thus, it is reasonable to propose that dioscin may offer similar therapeutic benefits.

It is noteworthy that under basal conditions, both adenyl/guanyl cyclase activity and PDE activity in resting platelets are maintained at low levels, resulting in a stable equilibrium with minimal production and degradation of cyclic nucleotides. Therefore, dioscin treatment alone may not significantly alter cAMP or cGMP levels due to the limited substrate available for PDE inhibition. However, upon stimulation with GPCR agonists such as U46619, cyclase activity increases, leading to enhanced production of cyclic nucleotides, while PDE activity also markedly rises to accelerate their breakdown. Under these activated conditions, dioscin's PDE inhibitory effect becomes functionally more pronounced, effectively elevating cAMP/cGMP levels, as demonstrated in Fig. 3. This context-dependent modulation aligns with previous studies reporting significant cyclic nucleotide accumulation only when PDE inhibition is combined with agonist-induced stimulation^{35,36}. These findings suggest that dioscin's antiplatelet mechanism is closely associated with its capacity to regulate PDE activity and cyclic nucleotide signaling specifically under stimulated conditions, thereby influencing downstream pathways such as VASP and IP₃R phosphorylation.

Pathways involved in signaling, such as the PI3K/Akt and MAPK cascades, are crucial for platelet function^{14,15}. For instance, in hyperglycemic animal models, p38 MAPK is activated in immune cells, including macrophages and dendritic cells, contributing to the development of atherosclerotic plaques. Dioscin has been shown to reverse the upregulation of p38 MAPK³⁷. Given its potential to reduce atherosclerosis, researchers have investigated whether dioscin exhibits similar inhibitory mechanisms in human platelets. Mei-Chi et al. have demonstrated that the phosphorylation of MAPK proteins (p38, ERK, and JNK) is essential for the production of

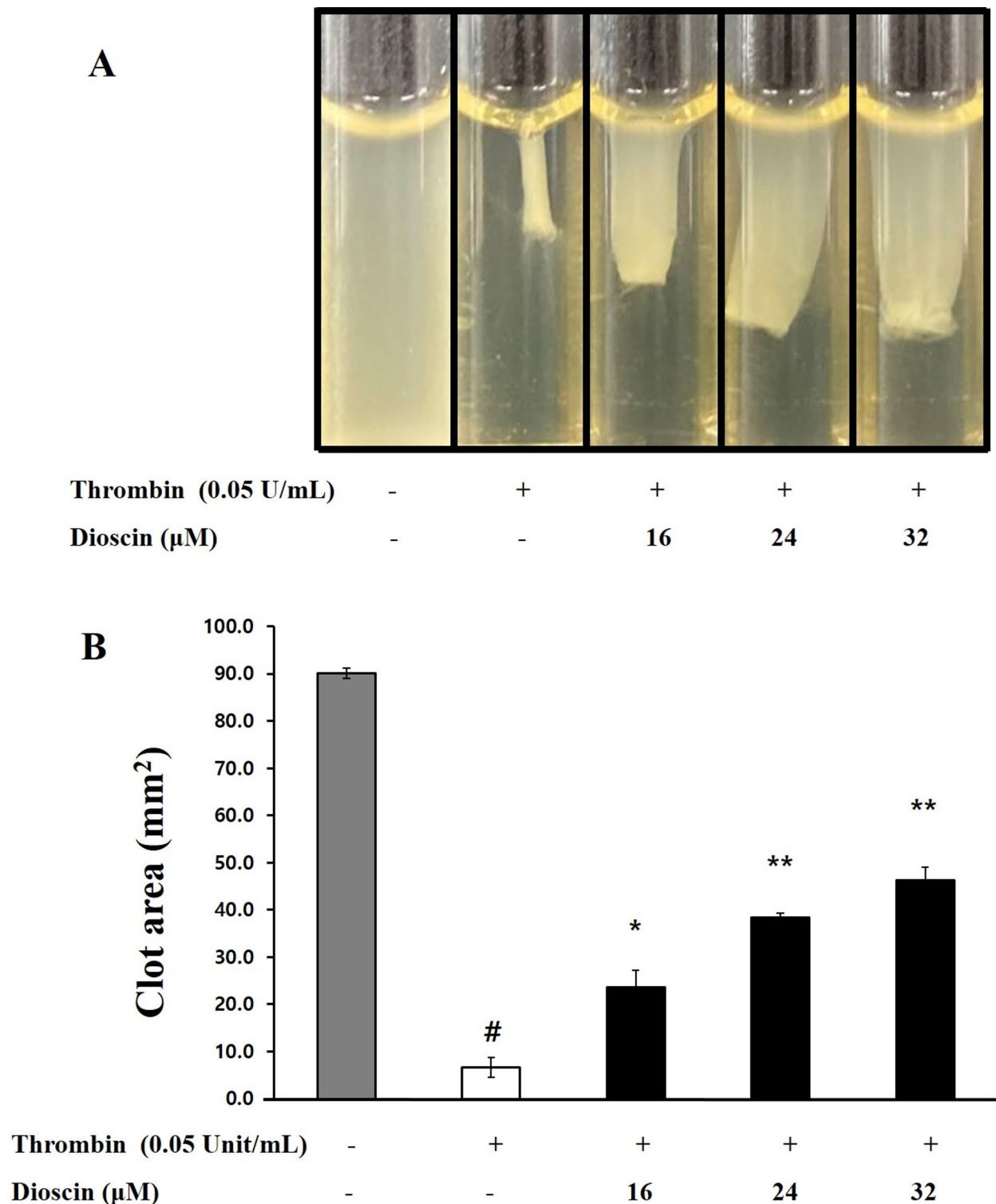


Fig. 7. Dioscin's influence on platelet-mediated clot retraction assay. **(A)** Dioscin's effect on fibrin clots retracted by thrombin. **(B)** Dioscin's impact on the area of thrombin-retracted fibrin clots. Data are represented as mean \pm SD ($n=4$). Statistical significance is indicated by # $p < 0.05$ in comparison to non-stimulated platelets, * $p < 0.05$, ** $p < 0.01$ and *** $p < 0.001$ when compared to U46619-stimulated platelets.

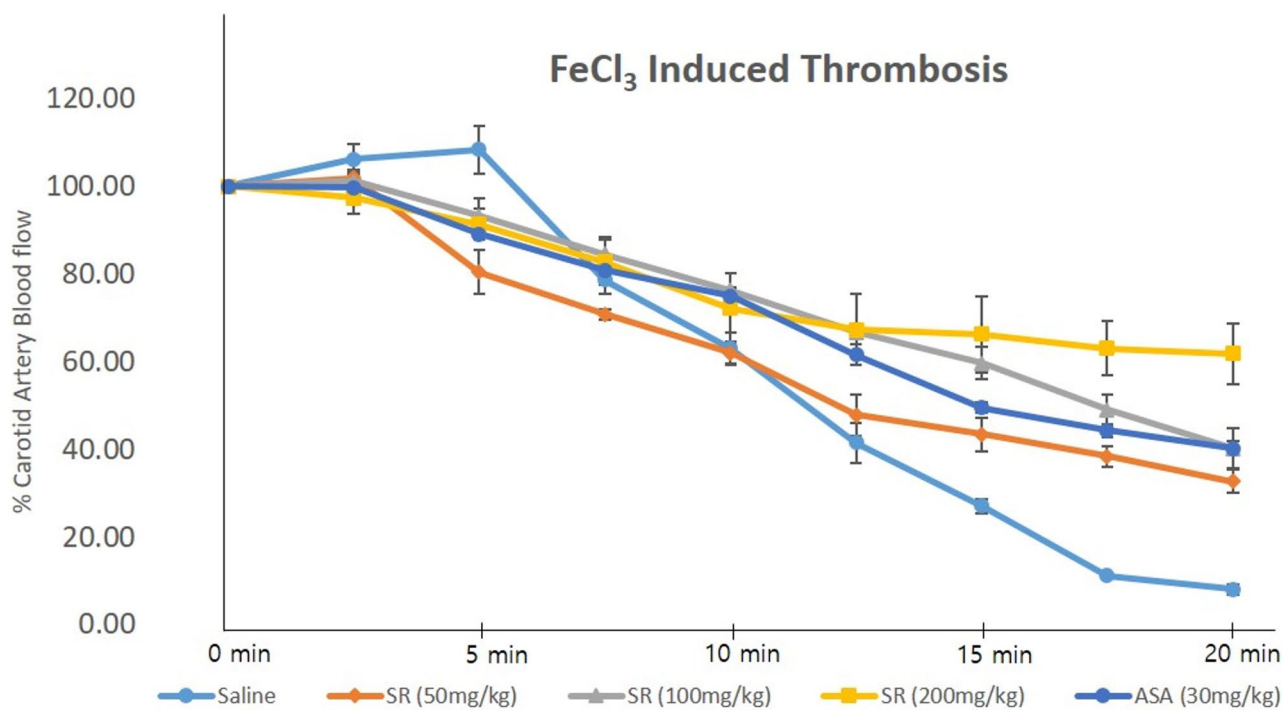


Fig. 8. Anti-thrombotic effects of *Smilax china* rhizomes extract containing dioscin (SR) on FeCl₃-induced thrombosis model. Data are represented as mean ± SD (n = 5). Each group of rats was orally administered SR and aspirin at each concentration for 7 days prior to FeCl₃ exposure.

Treatment	Dose (mg/kg)	Blood flow rate (%)		
		10 min	15 min	20 min
Saline	0	62.99 ± 3.52	26.99 ± 1.60	8.09 ± 1.20
SR	50mg/kg	61.92 ± 2.60	43.39 ± 3.76**	32.72 ± 2.68***
	100mg/kg	76.21 ± 0.79	59.62 ± 3.69***	40.15 ± 4.58***
	200mg/kg	72.10 ± 0.79	66.20 ± 8.77***	61.85 ± 6.93***
Aspirin	30 mg/kg	74.39 ± 1.39	49.53 ± 1.23***	40.23 ± 1.69***

Table 1. Effects of *Smilax china* rhizomes extract containing dioscin (SR) on blood flow of FeCl₃-induced thrombosis model. Each group of rats was orally administered SR and aspirin at each concentration for 7 days prior to FeCl₃ exposure, and the results at 10, 15, and 20 min after FeCl₃ exposure were presented (n = 5). *p < 0.05, **p < 0.01, and ***p < 0.001 from vehicle control (saline).

thromboxane A₂ (TXA₂), a potent autocrine factor that promotes platelet aggregation by triggering arachidonic acid release and increasing cPLA₂ phosphorylation³⁸. This makes TXA₂ a key marker for assessing the efficacy of compounds that inhibit platelet activity³⁸.

The study revealed that dioscin caused a substantial inhibition of U46619-induced platelet aggregation, with the effect being dependent on the concentration used. Furthermore, it significantly reduced the release of serotonin, ATP, and TXA₂, which serve as markers for granule secretion within the cell, as well as P-selectin expression, further confirming its inhibitory effect on platelet activation.

In addition, dioscin strongly inhibited the phosphorylation of key signaling proteins, including PI3K/Akt, MAPK (p38 and JNK) and cPLA₂. By targeting these pathways, dioscin effectively blocked the release of intracellular granules, preventing further platelet aggregation. Similarly, artocarpesin, a flavonoid from *Cudrania tricuspidata*, exhibited comparable antiplatelet activity. It influences several signaling processes by inhibiting aggregation triggered by U46619, reducing calcium mobilization, suppressing glycoprotein IIb/IIIa activation, and preventing clot contraction initiated by thrombin. Additionally, it enhances VASP and IP3R phosphorylation while reducing the activities of p38, JNK, and PI3K/Akt³⁹.

Additionally, integrin αIIbβ₃ activation and granule release are crucial components in signal transduction, which regulates platelet cytoskeletal remodeling and plays a key role in platelet aggregation and thrombus formation. This process is vital for repairing damaged blood vessels. Activated platelets gather at injury sites, binding to fibrin to form thrombi. Fibrin clot contraction usually occurs within 30–60 min, relying heavily on the interaction between fibrinogen and integrin αIIbβ₃. By inhibiting αIIbβ₃, platelets mediated clot retraction

can be slowed or prevented⁴⁰. Thrombin, a major factor in the coagulation process, activates integrin $\alpha\text{IIb}\beta_3$ on platelets, which increases fibrinogen binding and promotes clot formation. Flavonoids, known for their cardiovascular benefits, have been explored for their antithrombotic properties, potentially linked to their interactions with cellular receptors⁴¹. Certain flavonoids may have the ability to reduce platelet aggregation through their antithrombotic activity^{42–44}. In this study, dioscin significantly reduced thrombin-induced fibrin clot retraction in a manner dependent on concentration, suggesting that it has potent antiplatelet properties capable of delaying or preventing thrombus formation.

There are few previous studies that can serve as a basis for the pharmacodynamics of dioscin. Li K et al. (2005) only confirmed the pharmacokinetic changes of dioscin when administered intravenously at a dose of 1.0 mg/kg, and the maximum plasma concentration (C_{max}) of dioscin was approximately 31.1 nM⁴⁵. In comparison, the dioscin used in our in vitro study was considerably higher. The higher concentration was set to clearly observe the drug effect in vitro, and although the in vitro effect has limitations in directly comparing it with physiologically achievable concentrations, it is used as an important approach to evaluate the basic activity of the drug. Previous studies have shown that the oral bioavailability of dioscin is very low (0.2%), which means that the absorbed drug may have limited effects⁴⁵. However, dioscin has been observed to be delayed in the intestine and slowly eliminated from the tissues. These pharmacodynamic properties suggest that dioscin may exert its effects over a long period of time in vivo⁴⁵. In vivo carotid blood flow measurement experiments in the FeCl_3 -induced thrombosis model performed in this study demonstrated the antithrombotic effect in rats administered orally 50–200 mg/kg of *S. china* rhizomes extract (SR). Despite the low content and bioavailability of dioscin in SR, it should be considered that its antithrombotic effect may be mediated through conversion to diosgenin, an active metabolite with relatively high bioavailability (6%), or through accumulation in tissues⁴⁶. The antiplatelet and antithrombotic effects of diosgenin have been previously reported⁴⁷. In addition to dioscin, which is known as a representative physiological functional substance, SR is known to contain phenolic compounds such as catechin, afzelechin, astilbin, engeletin, and quercetin, and saponin components such as prosapogenins, parillin, and smilaspoin^{47–50}. Because these components may have synergistic effects and affected the antiplatelet effect, It is important to note that it is difficult to attribute the results observed in the animal model of thrombosis fed SR to dioscin alone. Nevertheless, these results support the potential of dioscin as an effective antithrombotic agent under physiological conditions. Future studies should focus on conducting in vivo experiments using pure dioscin to clearly confirm its independent action and efficacy, discovering *S. china* extracts with high dioscin content, and improving drug delivery systems or optimizing administration routes to further enhance clinical applicability. This study is expected to provide important insights into the future potential development of dioscin as an antithrombotic agent.

In conclusion, dioscin induces IP_3R phosphorylation by increasing cAMP/cGMP levels in human platelets, thereby preventing Ca^{2+} mobilization and inhibiting the binding between integrin $\alpha\text{IIb}\beta_3$ and fibrinogen by promoting VASP phosphorylation. In addition, dioscin exhibits antiplatelet activity by regulating phosphorylation of PI3K/Akt and MAPK. Dioscin significantly inhibited thrombin-induced clot retraction. Based on these findings, dioscin has potential antiplatelet effects that can delay or halt thrombus formation and exhibit strong efficacy as an antithrombotic compound.

Data availability

The original contributions presented in the study are included in the article, further inquiries can be directed to the corresponding author.

Received: 16 October 2024; Accepted: 27 June 2025

Published online: 15 July 2025

References

1. Tsao, C.W., Aday, A.W., Almarazooq, Z.I., Anderson, C.A.M., Arora, P., Avery, C.L., Baker-Smith, C.M., Beaton, A.Z., Boehme, A.K., Buxton, A.E., Commodore-Mensah, Y., Elkind, M.S.V., Evenson, K.R., Eze-Nliam, C., Fugar, S., Generoso, G., Heard, D.G., Hiremath, S., Ho J.E., Kalani, R., Kazi, D.S., Ko, D., Levine, D.A., Liu, J., Ma, J., Magnani, J.W., Michos, E.D., Mussolino, M.E., Navaneethan, S.D., Parikh, N.I., Poudel, R., Rezk-Hanna, M., Roth, G.A., Shah, N.S., St-Onge, M.P., Thacker, E.L., Virani, S.S., Voeks, J.H., Wang, N.Y., Wong, N.D., Wong, S.S., Yaffe, K. & Martin, S.S. American heart association council on epidemiology and prevention statistics committee and stroke statistics subcommittee. Heart disease and stroke statistics-2023 update: a report from the american heart association. *Circulation*. 147, 93–621 (2023).
2. Schwarz, U. R., Walter, U. & Eigenthaler, M. Taming platelets with cyclic nucleotides. *Biochem Pharmacol* **9**, 1153–1161 (2001).
3. Cavallini, L., Coassin, M., Borean, A. & Alexandre, A. Prostacyclin and sodium nitroprusside inhibit the activity of the platelet inositol 1,4,5-trisphosphate receptor and promote its phosphorylation. *J Biol Chem*. **271**, 5545–5551 (1996).
4. Laurent, V. et al. Role of proteins of the Ena/VASP family in actin-based motility of *Listeria monocytogenes*. *J Cell Biol*. **144**, 1245–1258 (1999).
5. Sudo, T., Ito, H. & Kimura, Y. Phosphorylation of the vasodilator-stimulated phosphoprotein (VASP) by the anti-platelet drug, cilostazol, in platelets. *Platelets* **14**, 381–390 (2003).
6. Irfan, M. et al. Ginsenoside-Rp3 inhibits platelet activation and thrombus formation by regulating MAPK and cyclic nucleotide signaling. *Vascul Pharmacol*. **109**, 45–55 (2018).
7. Adam, F., Kauskot, A., Rosa, J. P. & Bryckaert, M. Mitogen-activated protein kinases in hemostasis and thrombosis. *J Thromb Haemost*. **6**, 2007–2016 (2008).
8. Bugaud, F., Nadal-Wollbold, F., Lévy-Toledano, S., Rosa, J. P. & Bryckaert, M. Regulation of c-jun-NH₂ terminal kinase and extracellular-signal regulated kinase in human platelets. *Blood* **94**, 3800–3805 (1999).
9. Kramer, R. M., Roberts, E. F., Striffler, B. A. & Johnstone, E. M. Thrombin induces activation of p38 MAP kinase in human platelets. *J Biol Chem*. **270**, 27395–27398 (1995).
10. Nadal-Wollbold, F. et al. Platelet ERK₂ activation by thrombin is dependent on calcium and conventional protein kinases C but not Raf-1 or B-Raf. *FEBS Lett*. **531**, 475–482 (2002).
11. Michelson, A. D. Antiplatelet therapies for the treatment of cardiovascular disease. *Nat Rev Drug Discov*. **9**, 154–169 (2010).

12. Flevaris, P. et al. Two distinct roles of mitogen-activated protein kinases in platelets and a novel Rac1-MAPK-dependent integrin outside-in retractile signaling pathway. *Blood* **113**, 893–901 (2009).
13. Kramer, R. M. et al. p38 mitogen-activated protein kinase phosphorylates cytosolic phospholipase A₂ (cPLA₂) in thrombin-stimulated platelets. Evidence that proline-directed phosphorylation is not required for mobilization of arachidonic acid by cPLA₂. *J. Biol. Chem.* **271**, 27723–27729 (1996).
14. McNicol, A. & Shibou, T. S. Translocation and phosphorylation of cytosolic phospholipase A₂ in activated platelets. *Thromb Res.* **92**, 19–26 (1998).
15. Chuang, W. Y., Kung, P. H., Kuo, C. Y. & Wu, C. C. Sulforaphane prevents human platelet aggregation through inhibiting the phosphatidylinositol 3-kinase/Akt pathway. *Thromb Haemost.* **109**, 1120–1130 (2013).
16. He, S. et al. Dioscin promotes prostate cancer cell apoptosis and inhibits cell invasion by increasing SHP1 phosphorylation and suppressing the subsequent MAPK signaling pathway. *Front Pharmacol.* **11**, 1099 (2020).
17. Cui, L. et al. Dioscin elicits anti-tumour immunity by inhibiting macrophage M₂ polarization via JNK and STAT₃ pathways in lung cancer. *J Cell Mol Med.* **24**, 9217–9230 (2020).
18. Liu, W. et al. Dioscin inhibits stem-cell-like properties and tumor growth of osteosarcoma through Akt/GSK₃/β-catenin signaling pathway. *Cell Death Dis.* **9**, 343 (2018).
19. Hsieh, M. J., Tsai, T. L., Hsieh, Y. S., Wang, C. J. & Chiou, H. L. Dioscin-induced autophagy mitigates cell apoptosis through modulation of PI3K/Akt and ERK and JNK signaling pathways in human lung cancer cell lines. *Arch Toxicol.* **11**, 1927–1937 (2013).
20. Lee, C. D., Uy, N. P., Lee, Y., Lee, D. H. & Lee, S. Comparative analysis of phytochemical composition and antioxidant properties of *Smilax china* rhizomes from different regions. *Horticulturae*. **10**, 850 (2024).
21. Ko, S. N. et al. The inhibitory effects of *Glycyrrhiza uralensis* on human platelet aggregation and thrombus formation. *Biomed. Sci. Lett.* **29**, 242–248 (2023).
22. Grynkiewicz, G., Poenie, M. & Tsien, R. Y. A new generation of Ca²⁺ indicators with greatly improved fluorescence properties. *J Biol Chem.* **260**, 3440–3450 (1985).
23. Shin, J. H., Kwon, H. W., Rhee, M. H. & Hwa-Jin Park, H. J. Inhibitory effects of total saponin korean red ginseng on thromboxane A₂ production and p-selectin expression via suppressing mitogen-activated protein kinases. *Biomed. Sci. Lett.* **23**, 310–320 (2017).
24. Irfan, M. et al. Gintonin modulates platelet function and inhibits thrombus formation via impaired glycoprotein VI signaling. *Platelets* **30**, 589–598 (2019).
25. McNicol, A. & Jackson, E. C. Inhibition of the MEK/ERK pathway has no effect on agonist-induced aggregation of human platelets. *Biochem. Pharmacol.* **65**, 1243–1250 (2003).
26. Berridge, M. J. & Irvine, R. F. Inositol phosphates and cell signalling. *Nature* **341**, 197–205 (1989).
27. Nishikawa, M., Tanaka, T. & Hidaka, H. Ca²⁺-calmodulin-dependent phosphorylation and platelet secretion. *Nature* **287**, 863–865 (1980).
28. Kuo, J. F. et al. Calcium-dependent protein kinase: widespread occurrence in various tissues and phyla of the animal kingdom and comparison of effects of phospholipid, calmodulin, and trifluoperazine. *Proc. Natl. Acad. Sci.* **77**(12), 7039–7043 (1980).
29. Schwarz, U. R., Walter, U. & Eigenthaler, M. Taming platelets with cyclic nucleotides. *Biochem. Pharmacol.* **62**, 1153–1161 (2001).
30. Wentworth, J. K., Pula, G. & Poole, A. W. Vasodilator-stimulated phosphoprotein (VASP) is phosphorylated on Ser¹⁵⁷ by protein kinase C-dependent and -independent mechanisms in thrombin-stimulated human platelets. *Biochem J.* **393**, 555–564 (2006).
31. Napeñas, J. J. et al. Review of postoperative bleeding risk in dental patients on antiplatelet therapy. *Oral Surg Oral Med Oral Pathol Oral Radiol.* **115**, 491–499 (2013).
32. Gao, J. et al. Identification and characterization of phosphodiesterases that specifically degrade 3'3'-cyclic GMP-AMP. *Cell. Res.* **25**, 539–550 (2015).
33. Haslam, R. J., Dickinson, N. T. & Jang, E. K. Cyclic nucleotides and phosphodiesterases in platelets. *Thromb Haemost.* **82**, 412–423 (1999).
34. Menshikov, MYu., Ivanova, K., Schaefer, M., Drummer, C. & Gerzer, R. Influence of the cGMP analog 8-PCPT-cGMP on agonist-induced increases in cytosolic ionized Ca²⁺ and on aggregation of human platelets. *Eur. J. Pharmacol.* **245**, 281–284 (1993).
35. Cho, H. J. et al. Inhibition of platelet aggregation by chlorogenic acid via cAMP and cGMP-dependent manner. *Blood Coagul Fibrinolysis.* **23**(7), 629–635. <https://doi.org/10.1097/MBC.0b013e3283570846> (2012).
36. Lee, D. H. et al. Antiplatelet effects of caffeic acid due to Ca(2+) mobilizationinhibition via cAMP-dependent inositol-1, 4, 5-trisphosphate receptor phosphorylation. *J Atheroscler Thromb.* **21**(1), 23–37. <https://doi.org/10.5551/jat.18994> (2014).
37. Li, Y., Li, Y., Yang, T. & Wang, M. Dioscin attenuates oxLDL uptake and the inflammatory reaction of dendritic cells under high glucose conditions by blocking p38 MAPK. *Mol Med Rep.* **21**, 304–310 (2020).
38. Cipollone, F. et al. Differential suppression of thromboxane biosynthesis by indobufen and aspirin in patients with unstable angina. *Circulation* **96**, 1109–1116 (1997).
39. Kwon, H. W., Irfan, M., Lee, Y. Y., Rhee, M. H. & Shin, J. H. Artocarpin acts on human platelet aggregation through inhibition of cyclic nucleotides and MAPKs. *Appl. Biol. Chem.* **65**, 1–11 (2022).
40. Calderwood, D. A. Integrin activation. *J Cell Sci.* **117**, 657–666 (2004).
41. Landolfi, R., Mower, R. L. & Steiner, R. Modification of platelet function and arachidonic acid metabolism by bioflavonoids: structure-function relations. *Biochem. Pharmacol.* **33**, 1525–1530 (1984).
42. Lee, D. H. Antithrombotic effect of artemisinin through phosphoprotein regulation in U46619-induced platelets. *Biomed. Sci. Lett.* **29**, 184–189 (2023).
43. Yoon, S. S. et al. Anti-thrombotic effects of artesunate through regulation of cAMP and PI3K/MAPK pathway on human platelets. *Int. J. Mol. Sci.* **23**, 1586 (2022).
44. Lee, D. H. Inhibitory effect of scopoletin on U46619-induced platelet aggregation through regulation of Ca²⁺ mobilization. *Biomed Sci Lett.* **25**, 123–130 (2019).
45. Li, K., Tang, Y., Fawcett, J. P., Gu, J. & Zhong, D. Characterization of the pharmacokinetics of dioscin in rat. *Steroids* **70**, 525–530 (2005).
46. Wang, D. & Wang, X. Diosgenin and its analogs: potential protective agents against atherosclerosis. *Drug Des. Devel. Ther.* **16**, 2305–2323 (2022).
47. Joo, J. H. et al. Antimicrobial activity of smilax china L. root extracts against the acne-causing bacterium, cutibacterium acnes, and its active compounds. *Molecules* **27**, 23 (2022).
48. Feng, H. et al. The flavonoid-enriched extract from the root of Smilax china L. inhibits inflammatory responses via the TLR-4-mediated signaling pathway. *J Ethnopharmacol.* **256**, 112785 (2020).
49. Shao, B. et al. Steroidal saponins from Smilax china and their anti-inflammatory activities. *Phytochemistry* **68**, 623–630 (2007).
50. Wang, M. et al. Smilax china L.: A review of its botany, ethnopharmacology, phytochemistry, pharmacological activities actual and potential applications. *J Ethnopharmacol.* **318**, 116992 (2024).

Acknowledgements

This study was supported by a grant from the National Research Foundation of Korea, funded by the Korean government (Grant No. NRF-2022R1F1A1066551).

Author contributions

GHL: Conceptualization, Methodology, Writing-Original draft preparation. JPL and NH: Data curation, Formal analysis. CDL and GK: Visualization, Investigation. AAW: Methodology, Data curation. MHR: Data curation, Formal analysis. SL: Validation, Writing-Reviewing and Editing. DHL: Supervision, Writing- Reviewing and Editing, Funding acquisition.

Declarations

Competing interests

The authors declare no competing interests.

Additional information

Correspondence and requests for materials should be addressed to S.L. or D.-H.L.

Reprints and permissions information is available at www.nature.com/reprints.

Publisher's note Springer Nature remains neutral with regard to jurisdictional claims in published maps and institutional affiliations.

Open Access This article is licensed under a Creative Commons Attribution-NonCommercial-NoDerivatives 4.0 International License, which permits any non-commercial use, sharing, distribution and reproduction in any medium or format, as long as you give appropriate credit to the original author(s) and the source, provide a link to the Creative Commons licence, and indicate if you modified the licensed material. You do not have permission under this licence to share adapted material derived from this article or parts of it. The images or other third party material in this article are included in the article's Creative Commons licence, unless indicated otherwise in a credit line to the material. If material is not included in the article's Creative Commons licence and your intended use is not permitted by statutory regulation or exceeds the permitted use, you will need to obtain permission directly from the copyright holder. To view a copy of this licence, visit <http://creativecommons.org/licenses/by-nc-nd/4.0/>.

© The Author(s) 2025